Journal of Marine Research, 43, 163–178, 1985

Acoustical patchiness of mesopelagic micronekton

by Charles F. Greenlaw[1] and William G. Pearcy[2,3]

ABSTRACT

Patterns of acoustical scattering in both depth and horizontal extent were analyzed to estimate the spatial and temporal scales of variability in biomass of mesopelagic sound scatterers, principally micronekton. The patterns observed included extensive layers of low and nearly uniform scattering strength and distinct three-dimensional patches of stronger scattering. These patches dispersed vertically at night after diel migration of a portion of the scatterers, but reassembled quite accurately the following day. Analysis of variance spectra for average acoustical scattering profiles within a patch suggest that micro-patches, with dimensions on the order of 15 m vertically by 1 km horizontally, are present both day and night. Horizontal variance spectra suggest the possibility of different horizontal aggregation mechanisms at scales above and below approximately 8.9 km.

1. Introduction

Inhomogeneous distributions of organisms are common in the ocean. Many studies reveal patchiness of zooplankton and phytoplankton (e.g., Steele, 1978) over scales from centimeters to kilometers. Haury *et al.* (1978) used the Stommel Diagram as a model to classify horizontal spatial scales ranging from micro-scale (dimensions of 1 cm to 1 m) to mega-scale (>3000 km). They thought that ecological interactions occur between nektonic predators and zooplanktonic prey on the coarse scale (1–100 km) and significant changes in spatial structure might be related to the tolerable interval between successful hunts for food—on the order of a few days. If these scales apply to mesopelagic micronekton as well, investigation of the structure of a mesopelagic community would require sampling a region on the order of 100 km by 100 km in a matter of a few days. This would pose a formidable problem for net sampling. When the scales of vertical structure and diel effects are included, the number of net samples necessary can become prohibitive.

Acoustical estimation of the spatial patterns of mesopelagic micronekton over these scales, however, is feasible. Using appropriate acoustic frequencies for the predominant sizes of organisms, scattering strengths can be used to estimate total biomass of the dominant sound scatterers (Greenlaw *et al.,* 1979), thus patterns of sound

1. Tracor Inc., P.O. Box 1119, Philomath, Oregon, 97370, U.S.A.
2. School of Oceanography, Oregon State University, Corvallis, Oregon, 97331, U.S.A.
3. Reprint requests should be addressed to Dr. Pearcy.

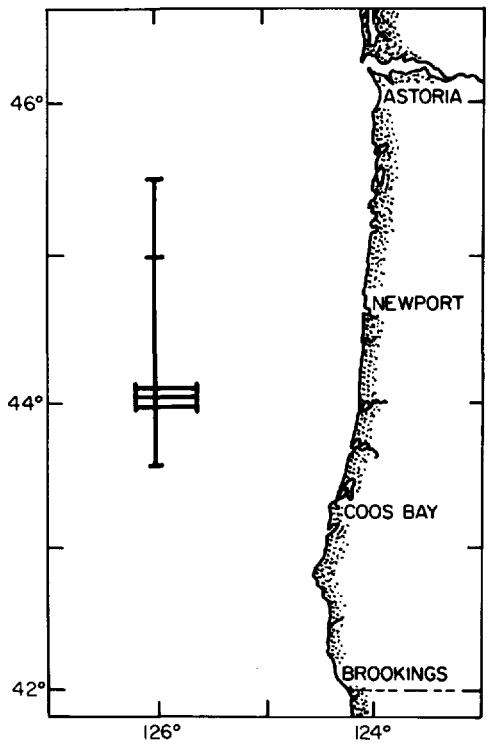

Figure 1. Area of acoustical transects. North-south transects were made along 126W, in waters 3000 m deep. Short transects were made across this line at the latitudes marked. Currents were from the north during these measurements.

scattering can be used to infer the spatial patterns of the scatterers. Details of the structure such as species composition cannot be determined acoustically but acoustical measures of gross structure would allow direction of net sampling to more efficiently estimate these properties.

The work reported here is an effort to measure the spatial and temporal scales of mesopelagic micronekton off Oregon. The goals of this experiment were (1) to estimate the spatial scales, vertically and horizontally, of the sound scattering and (2) to determine, if possible, whether the patterns were persistent over several diel cycles.

2. Data collection

A research cruise explored the spatial pattern of sound scattering during 18–26 August, 1982, about 135 km offshore of Newport, Oregon, where water depths are about 3000 m. Most of the acoustical data were collected during linear transects along 126W, along and against the prevailing currents. Tracklines of the transects are shown in Figure 1. Transects along latitudes were conducted on 25 August, providing a modicum of data across the prevailing current. Day-time transects were obtained on 5

days: 19–21 August, 23 August, and 25 August. A night-time transect was made on the night of 20–21 August over the trackline followed on 20 and 21 August.

Acoustical scattering data were obtained using a special echosounder system consisting of a towed body containing the transducer(s), a 2 KW power amplifier, a custom heterodyne receiver with a 20 log R time-varied-gain, and a micro-computer to control the system and store the digitized echo data. Echo data were stored in the form of average echo profiles—similar to the operation of a signal averager—over a selected number of pings. Echoes were sampled at fixed depths and these samples summed over successive pings. Each depth sample thus consisted of the sum of echo values arising from scattering at a fixed depth. The echo processor stored average profiles of echo amplitudes, echo intensities, and squared echo intensities to allow inspection of the first few moments of the echo statistics but, for these purposes, only the average echo intensities were analyzed. The number of pings per average profile was set at 64. At a nominal ships speed of 3 m/sec, each profile represents an average over about 500 m horizontal distance. The data presented here were taken at a frequency of 20 kHz.

Prior to analyzing the acoustic data, the profiles were converted to volume backscattering coefficients, sv. The volume backscattering coefficient is the ratio of backscattered intensity from a unit volume of water containing scatterers to the intensity incident on that volume, referred to unit distance from the volume (Urick, 1967). The volume scattering strength, Sv, is defined as 10 log (sv). This unit is commonly used in acoustical literature. If the distribution of scatterers within the insonified volume is uniform-random (three-dimensional Poisson), the volume backscattering coefficient is proportional to the number of scatterers per unit volume. The proportionality constant is the backscattering coefficient for an average scatterer. This constant is a function of the distribution of scatterer types and sizes; at 20 kHz it is somewhat sensitive to differing distributions of swimbladder bubble sizes. Thus, differences in sv or Sv from place to place may signify changes in the number of scatterers and/or changes in the distribution of scatterer types, sizes, or swimbladder sizes. Fishes, especially those with gas-filled swimbladders, are much stronger scatterers than zooplankton at any frequency. The relatively low frequency we used tends to de-emphasize the scattering contributed by smaller, nonresonant scatterers such as zooplankton. Thus, the scattering is presumed to arise largely from fishes and other micronekton.

Gross structure of the sound scattering patterns was analyzed using contour maps of sound scattering versus depth and latitude/longitude (Figs. 2–3). Contour intervals were drawn at equal values of volume backscattering strength, Sv. If the changes in volume backscattering strength are interpreted as changes in the biomass of scatterers, an increase of 10 dB in Sv represents a ten-fold increase in biomass of scatterers. The contour intervals are 5 dB, which correspond roughly to factors of 3 in biomass. Since the variations in biomass are the subject of this study, we did not convert acoustical units to biomass units.

Estimates of spatial scales and variances were obtained from spectral analysis of the

volume backscattering coefficient records. The processing was similar to that employed by Greenblatt (1982). After selection of the data records for processing, the data were first-difference filtered (Jenkins and Watts, 1968) to produce sequences of changes in the volume backscattering coefficients. That is, the sampled value of sv at each depth was replaced by the difference between the sample at the next depth and the original sample. This processing removed the mean values of the data. Each data record was Fourier-transformed and the power spectrum (with corrections for the high-pass filter effects of the first-difference process) calculated. Since the input data consisted of changes in volume backscattering coefficients (with a zero mean), the power spectral levels are in units of squared differences or variance of the volume backscattering coefficients. Thus the spectra, referred to as variance spectra, represent estimates of the distribution of variance in the backscattering coefficient among spatial scales.

The sample intervals for the input data are 6 m vertically and ca. .5 km horizontally. The frequency axes for the power spectra are cycles per meter (depth variance spectra) or cycles per km (horizontal variance spectra). Fourier techniques decompose input records into constituent sinusoids at a set of frequencies determined by the sampling frequency and record length. A peak at some frequency, F, implies the presence of a strong sinusoidal variation with a period $T = 1/F$, where the period is a measure of the extent (usually time, spatial length in this case) encompassed by a complete cycle of the sinusoid. The width of the peak is a measure of the number of cycles of the sinusoid contained in the input record, becoming narrower as the record contains more cycles.

3. Gross structure and temporal persistence

The first transect, on 19 August, revealed a weak, relatively uniform single acoustical scattering layer extending ca. 65 km in a north-south direction (Fig. 2a). The median depth of this layer, judged by the -70 dB contours, was 325 m with an average thickness of about 75–100 m. Occasional "pockets" of stronger scattering (>-65 dB) occurred within and below the main scattering layer, but the general impression was of a more-or-less uniform scattering layer.

Considerable structure was found in the scattering layer on the following day, along a transect which extended ca. 124 km south of the starting point of the first transect (Fig. 2b). Strong scattering was observed south of 44.4N over broad depth intervals, implying ca. an order of magnitude more biomass in the southern than northern portions of this transect. Regions of strong scattering extended to ca. 500 m, much deeper than observed on the preceding day, probably because of higher solar irradiance on 20 August. Distinct variations in both depth and horizontal extent are seen in Figure 2b. The regions of strong scattering are connected by regions of lesser scattering of ca. 1/10 the intensity of the stronger scattering regions. Patches of strong scattering (>-60 dB) as small as 1 km across by ca. 15 m thick and as large as 30 km across by 100 m thick can be seen in the contour plot. Shapes are irregular and the patches

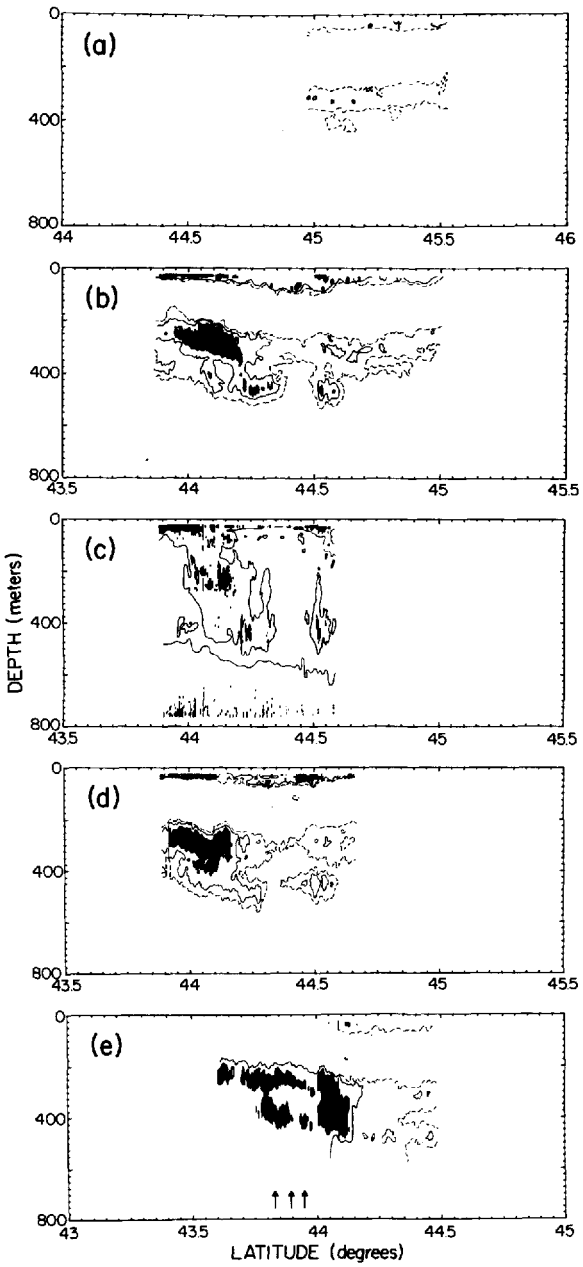

Figure 2. Contour maps of volume scattering strength versus depth and latitude. Contour intervals are 5 dB with dashed lines enclosing regions of Sv > -65 dB, solid lines enclosing regions of Sv > -60 dB, and vertical hatching in regions of Sv > -60 dB. Each plot represents data collected during a single day or night period; on 19 August 1982 (a), 20 August (b), the night of 20–21 August (c), 21 August (d), and 23 August (e). Currents setting generally to the south appear to explain the southerly shift of the pattern from 20 August to 21 August.

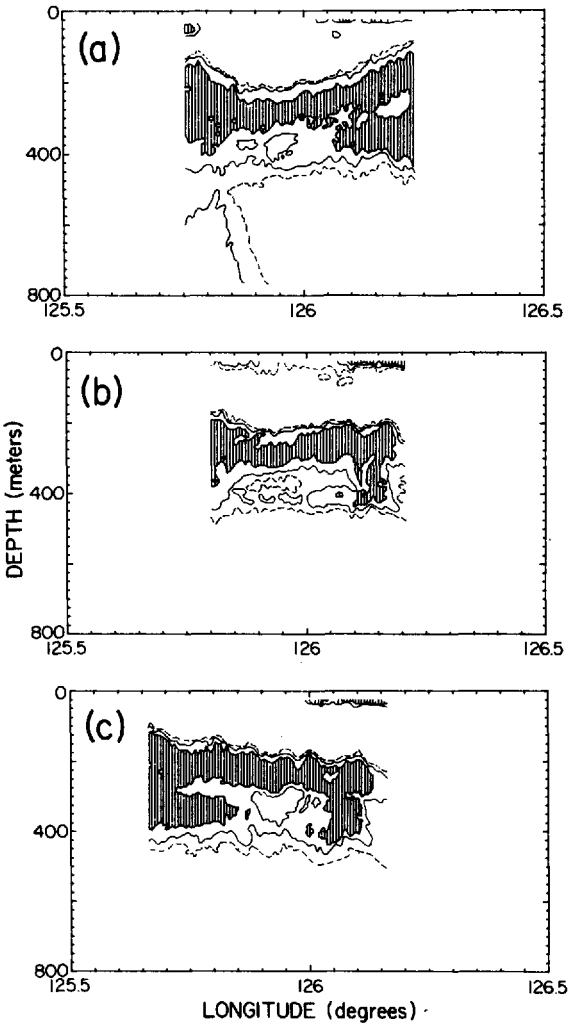

Figure 3. Contour maps of volume scattering strength versus depth and longitude. These data were taken in the region of strong scattering observed in north/south transects. Latitudes for the plots are: 44 00'N (a), 44 03'N (b), and 44 07'N (c).

appear to be randomly distributed, implying that a statistical measure of patchiness would by appropriate.

The day-time transect of 20 August was partially retraced (ca. 80 km) after sunset to observe the night-time structure after the migratory animals ascended from their day-time depths (Fig. 2c). Comparison of the night-time contours with the previous day-time contours shows considerable similarity in horizontal and vertical structure. The -65 dB contours bear a distorted, but recognizable, relationship to the day-time

contours, suggesting aggregations that maintained some cohesiveness. The scales of patchiness decreased at the higher contour levels (stronger scattering), both in depth and horizontal extent. The principal strong scattering patch appears to break up, with numerous small regions of strong scattering distributed irregularly from 450 m to the surface. Note the presence of strong scattering patches below 600 m. These are presumably migrators from depths greater than 800 m, not observed during the day-time transects.

On the following day, the transect was repeated again (Fig. 2d). The patterns strongly resembled those of the preceding day. The whole pattern appeared to have been transported some 5 km to the south, a net advection of ca. 6 cm/sec. This is a reasonable value for the currents in this region (Stevenson *et al.*, 1969). There was some indication of redistribution, in that the −70 dB contours were disconnected at about 44.4N, possibly due to advection of the pattern across the line of the transect.

This transect was repeated again during the day of 23 August. This scattering pattern (Fig. 2e) displays little similarity to previous transects, however. Again, cross-transect advection may explain the differences. This transect extended farther south than the preceding transects, approximately 20 km beyond the point to which the 21 August pattern would be advected. The beginnings of another strong patch can be seen at 43.7N. A leak developed in the transducer cable during this transect, coupling 60 Hz noise spikes from the ship's generator into the acoustic system. The result was a fairly abrupt increase in background noise levels, followed by a further gradual increase in noise during the remainder of the transect. This is seen in the contour plot as unrealistic lower depths for the −65 dB and −70 dB contours. Because the noise level was not constant during the transect, no corrections to the volume scattering strengths were possible. Thus, the −60 dB contours in this figure may overestimate true scattering levels.

On 25 August three short day-time transects were made at right angles to the line of the previous transects. Contour plots for these transects are shown in Figure 3. These plots demonstrate that variability is a three-dimensional spatial process. Although the lengths of these transects (32–39 km) were insufficient to allow measurement of the scales of horizontal spatial structure, the patterns are at least as complex across as along the prevailing current and the scales of variability appear to be similar.

4. Spatial scales

The estimates of gross structural scales obtained from the contours of Sv in the preceding section are strongly affected by the choice of contour intervals. Contour maps based upon finer intervals would produce an impression of greater fine-scale variability while contours at larger intervals would result in either larger or smaller estimates of patch size, depending upon the levels chosen. Also, the choice of logarithmic units (Sv) biases estimates toward large significant differences. To circumvent these problems and to enable quantitative estimation of the spatial scales of

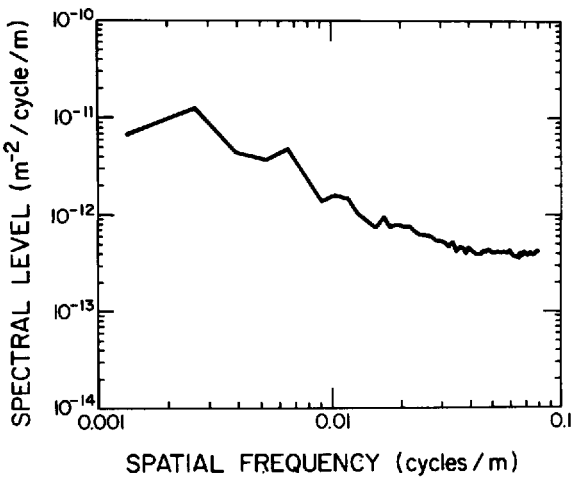

Figure 4. Spectrum of the variance of volume scattering coefficients in depth for the transect data of 19 August. This spectrum is the average of the spectra of 145 depth profiles. Maximum variance occurs on spatial scales (inverse of spatial frequency) corresponding to the depth and thickness of the main scattering layer. Note that small scale variance is only about an order of magnitude weaker than the large scale variance.

variability, variance spectra were calculated for both vertical and horizontal variations in the volume scattering coefficient.

a. Vertical variability. The depth-dependent variance spectrum shown in Figure 4 is an average of the spectra of 145 day-time scattering profiles taken on 19 August. Fourier analysis decomposes data records into constituent sinusoids, thus a spectral component at, say, .1 cycle/m implies a sinusoidal variation with a total wavelength of 10 m. At very small scales and, perhaps, for horizontal spectra, the variations might possibly be modelled as sinusoidal. The larger-scale patchiness tends to occur in lumps, however, which are at best half-sinusoids. The variance spectrum of a half-sinusoid of "length" L would have a peak at a spatial frequency of $1/2L$ since the wavelength of the fundamental-frequency sine wave is $2L$. Thus, a 5 m thick layer would appear as a spectral peak at .1 cycle/m. To emphasize the difference between spatial frequency and spatial lengths, we use the term "characteristic" length or scale to refer to dimensions of lumps. In Figure 4 there are peaks at characteristic scales of 77 m and 192 m, corresponding to the average thickness and depth of the layer respectively. (For the choice of sample interval and number of samples used to process these data, the resolution of characteristic scales is poor at large scales. Thus, the median depth of the layer is only poorly estimated.) The spectrum is "red," decreasing in level with increasing frequency (decreasing spatial scale). This is consistent with the general expectation that large changes in scattering intensity (or biomass) tend to occur over

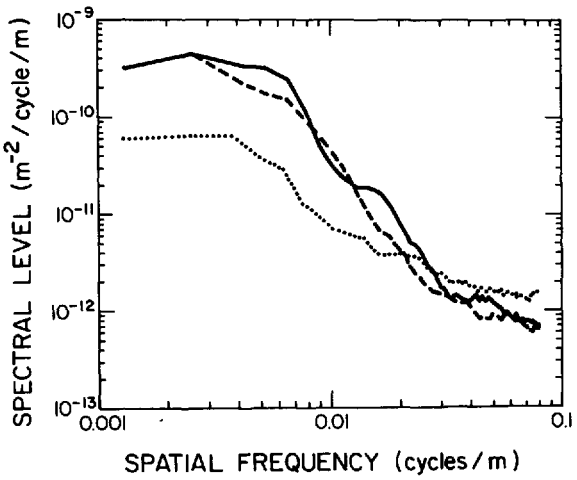

Figure 5. Depth variance spectra for the southernmost region of strong scattering as observed on 20 August (solid curve), the night of 20–21 August (dotted curve), and 21 August (dashed curve). Spectral variance at large scales decreases at night, reflecting the diffused structure caused by vertical migration. Note that the variance at smaller scales at night is comparable to the day-time levels, suggesting approximately equal levels of small scale variability both day and night. The similarity of the depth variance spectra on succeeding days implies similarity of the *statistical* measures of the depth distributions on these days.

large scales and smaller changes tend to occur over smaller scales (Greenblatt, 1982). The overall range of spectral values is only about one order of magnitude. We interpret this to mean that small-scale variability is relatively strong within this layer.

Figure 5 shows depth variance spectra for day and night records taken on 20–21 August. The scattering profiles used to calculate these spectra were selected to encompass approximately the southernmost feature observed in the contour plots. The solid curve is an average of 106 spectra from the 20 August day-time transect. The dotted line is the average of 106 spectra of the night-time repeat of this transect. These spectra are qualitatively similar to that of Figure 4, but the level of variance is much larger at all scales—reflecting stronger patchiness in scattering intensity in this region of stronger scattering. At the larger scales the night-time spectral levels are about an order of magnitude lower than the corresponding day-time values. This reduced scattering is consistent with the vertical spreading of the layer at night as seen in the contour plots (Fig. 2c). Spectral levels at smaller scales are approximately the same for day and night, however.

Day-time spectral variance is high and fairly uniform for characteristic scales greater than ca. 70 m, decreases with decreasing characteristic scales to ca. 17 m, and is relatively uniform to the smallest resolved scales (6 m). The small-scale variance is nearly 3 orders of magnitude lower than that at larger scales. Night-time spectral

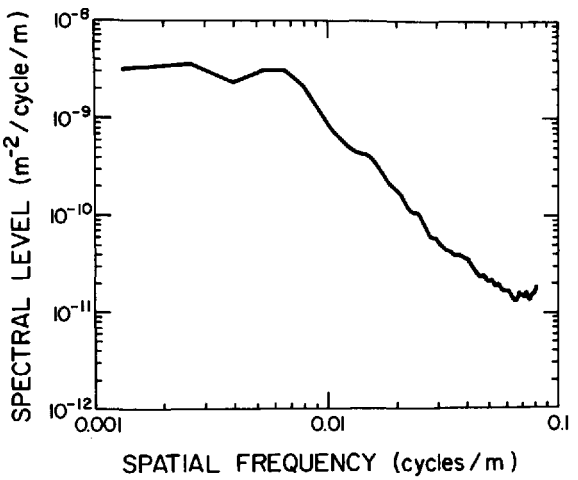

Figure 6. Depth variance spectrum for the east/west transects made on 25 August. Spectra from the three transects were averaged to produce a spectrum with approximately the same number of degrees of freedom as the north/south spectra. The shape of this spectrum is similar to those of Figure 5.

variance is qualitatively similar to the day-time spectrum; the major difference is lower variance at large characteristic scales.

The contour map for night-time structure (Fig. 2c) conveys the impression that a relatively large and homogeneous day-time patch had broken up into a number of smaller patches after the evening migration. If this impression were correct, one would expect that the variance spectrum would be high at small (less than ca. 20 m) characteristic scales. However, the night-time spectrum is only slightly higher than the day-time spectrum at high spatial frequencies. This suggests that small-scale patchiness is comparable day and night. The day-time layer is apparently composed of subpatches with characteristic scales similar to those observed at night. The dashed curve in Figure 5 is the depth-dependent variance spectrum for day-time measurements on 21 August. This spectrum is nearly identical to the spectrum for the preceding day, supporting the qualitative similarity of the patterns over a diel migration period noted previously.

Day-time depth spectra were also calculated from the cross-track transects of 25 August. The average of these spectra (Fig. 6) is very similar in shape to the spectra of 20 and 21 August but about an order of magnitude higher in level. The shift in overall level of the spectrum suggests that these data encompassed an aggregation with higher biomass than that measured on previous days. The similarity of the shapes of the spectra in Figures 4–6, however, implies that the vertical structure in this region is largely independent of total biomass and, further, that the average vertical structure of the patch as a whole is similar in the two orthogonal directions measured.

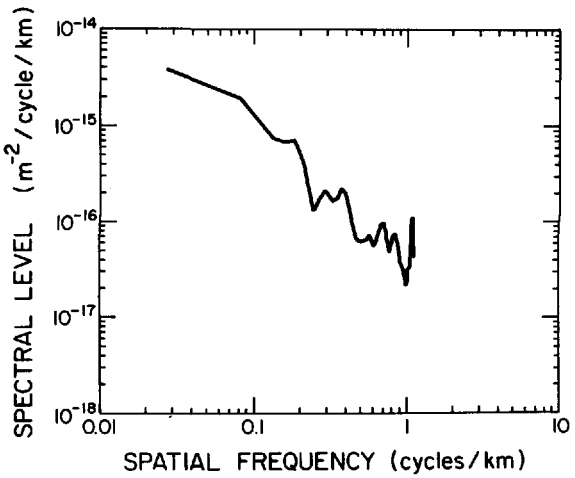

Figure 7. Spectrum of the variance in volume scattering coefficients over horizontal extent for the main layer observed on 19 August. Depth records were averaged over 275-375 m prior to spectral analysis. Note that the spatial frequency is cycles/km for this, and succeeding, plots and that the spectral levels are correspondingly scaled.

b. Horizontal variability. Variance spectra were also calculated to examine the scales of horizontal variability. Scattering intensities from each separate depth profile were averaged over 100 m depth intervals and input data files constructed from horizontal sequences of average scattering intensities. These files were then processed in the same fashion as the depth records. Input records were averaged over depth to reduce the effects of vertical structure; the resulting spectra were further smoothed by summing adjacent frequency values and by "Hanning" these spectra (Jenkins and Watts, 1968). This smoothing removed most of the high-frequency fluctuations in the spectra while retaining the average shape.

The horizontal variance spectrum for the main layer (275–375 m) on 19 August is shown in Figure 7. This spectrum is "red," like the depth spectra. Note that the abscissa is cycles/km for these plots and that the units for spectral level are correspondingly scaled. (Divide these spectral levels by 1000 to compare with the depth spectra.) Most of the horizontal variability in scattering intensity occurs on large scales, but the presence of distinct peaks in the spectrum at higher frequencies suggests the existence of smaller characteristic scales of aggregation. The peak at .19 cycles/km indicates patches with characteristic lengths of ca. 2.6 km. It is not evident whether or not this is significant. Peaks at .3–.4 cycles/km and .7–.85 cycles/km correspond to characteristic patch lengths of 1.2–2.7 km and .6–.7 km respectively. Structure at these scales would be difficult to extract from contour plots.

Horizontal variance spectra for four depth intervals of the 20 August transect are presented in Figure 8. The interesting feature of these spectra is the similarity of the

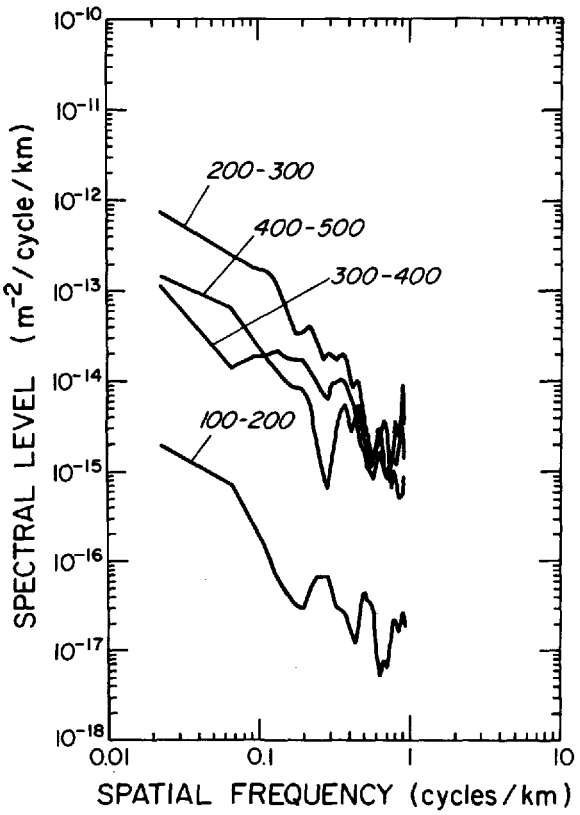

Figure 8. Horizontal variance spectra for the transect of 20 August. Depth profiles were averaged over 100 m intervals prior to spectral analysis (marked on plots). The entire transect (Fig. 2b) is included in these spectra.

variance spectra over the three deepest depth intervals (200–500 m). Variability in the 100–200 m depth range is more-or-less similar in structure to that of the deeper layer but the lower scattering strength is reflected in the lower overall spectral level. The shallow spectrum is also very similar to the spectrum from the main layer on 19 August (Fig. 7). No single characteristic scale is evident from these plots; rather, a range of scales is implied. Two features are noteworthy, however. First, all of the variance spectra for depths >200 m converge to a minima at a frequency of ca. .57 cycles/km (.9 km characteristic length). The differences between the spectra are larger at frequencies below this value, somewhat less at frequencies above this value. This suggests differences in the aggregation properties at scales greater than and less than ca. .9 km. Second, the spectral shapes at ca. .29 cycles/km (1.7 km characteristic length) vary from a distinct peak at 100–200 m, to a plateau at 200–300 m, to a sharp null at 300–400 m, and finally to a minor null at 400–500 m. The null at .57 cycles/km

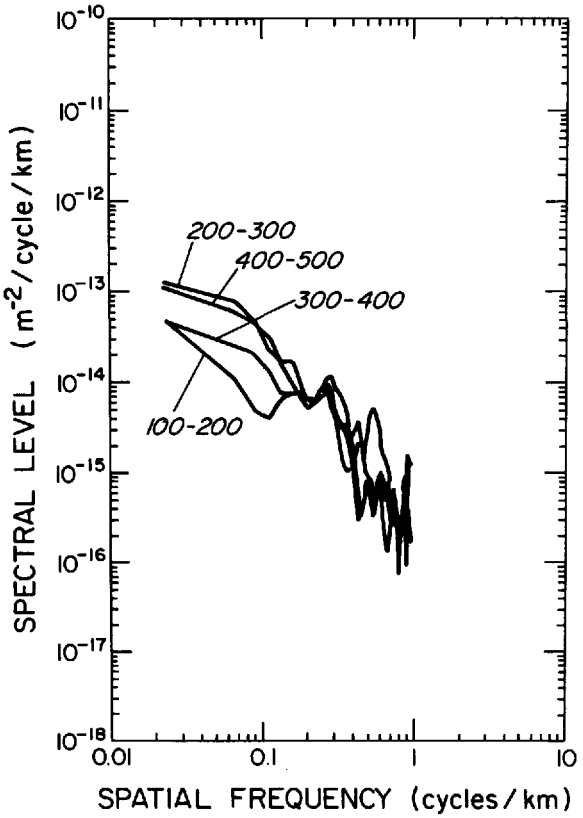

Figure 9. Horizontal variance spectra for the night-time transect of 20–21 August. Depth profiles were averaged over 100 m intervals prior to spectral analysis. Compare these spectra with the day-time spectra of Figure 8.

for depths >200 m is matched with a peak in the 100–200 m spectrum also. These trends suggest that horizontal and vertical structure may be coupled. Other than the spectral levels, these features are the major depth-dependent effects. Horizontal variance spectra for the following day-time transect were similar to these, with the same relationships between peaks and nulls over the various depths.

Figure 9 shows equivalent horizontal variance spectra for the night transect on 20–21 August. The vertical spreading seen in the contour plots appears to have homogenized the horizontal distributions over the depth range 100–500 m, reducing the differences in spectral levels at the different depth. Again, there is no single characteristic scale to the structure, although there is a minor peak at ca. .29 cycles/km at all depths. Overall, these spectra are quite similar in shape to the shallow (100–200 m) day-time spectra.

5. Discussion

Patches of strong scattering have been previously observed in oceanic waters off Oregon. They are quite common but not necessarily ubiquitous. The initial transect revealed a relatively uniform layer structure with an extent of 65 km. It would appear that inter-patch intervals on the order of the "coarse scale" of Haury *et al.* (1978) are likely. Structure in the patches is complex in both depth and horizontal extent and is three-dimensional (e.g., Figs. 2–3).

Patches persisted at least as long as a diel cycle. Similarity of the contour maps of scattering intensity over two consecutive days (Fig. 2b–2c) is an indication that the gross properties of the pattern are maintained after the upward dispersal of organisms following the evening migration. Similarity of the depth-dependent variance spectra for the patch on succeeding days (Fig. 5) is evidence that the structure was reproduced in a statistically similar fashion, with similar scales. Coupled with the gross similarity of the contour plots, this is strong evidence for similarity of the spatial pattern of sound scattering (and, we presume, biomass) over a diel cycle. From this, it can be inferred that the causal mechanism of aggregation for these organisms is not random. Moreover, the factors which contribute to aggregation are effective over scales ranging from 10's of m to 10's of km and over periods of one or more days.

The contour map of night-time scattering (Fig. 2c) displays numerous, small patches of strong scattering more-or-less randomly distributed throughout the depth extent of the southernmost feature. Comparing the day-time and night-time contours, it would appear that a relatively homogeneous, large day-time aggregation dispersed or broke up into smaller aggregations which migrated to various depths at night. If this interpretation were correct, small-scale (high frequency) variance should have increased substantially over that measured during the day. The actual variance spectra (Fig. 5) are very similar above ca. .025 cycles/m (characteristic scales smaller than ca. 20 m) both day and night, however. Variance at large scales (>20 m) decreases at night, reflecting the change from a relatively compact layer during the day to a broad distribution in depth at night. The minor change in variance at the small scales can be interpreted as evidence that the smaller-scale aggregations apparent in the night-time contour map were present in the main layer during the day-time as well; the coarse intervals of the contour maps mask their presence. The day-time horizontal variance spectra (Fig. 8) suggest the possibility of different aggregation mechanisms for scales above and below ca. 0.9 km, within the main layer. This may reflect a superposition of the micro-patches on a larger scale aggregation. (An analogous pattern occurs in northern anchovy distributions off California, where fish schools of variable size form loose groupings with pattern on larger scales; Hewitt *et al.*, 1976; Smith, 1978.) Apparent micro-patches were also observed on a previous cruise off Oregon (with D. V. Holliday) using a broadband acoustic system lowered into the main scattering layer. Qualitative estimates of the sizes of these patches were on the order of 10's of meters vertically by roughly a kilometer horizontally, in agreement with the scales

observed here. The frequency dependence of the echoes from these micro-patches was consistent with that expected from mesopelagic fishes with gas-filled swimbladders, the animals thought to be the major cause of low-frequency scattering layers off Oregon (Pearcy and Mesecar, 1971; Johnson, 1977; Pearcy, 1977).

Distributions of mesopelagic fishes are known to be clumped or patchy from net sampling (Pearcy, 1964; Atsatt and Seapy, 1974) and from submersible observations. Barham (1971) noted loose aggregations and "swarms" of lanternfishes from submersible dives off the west coast of North America. One of us (WGP) observed distinct aggregations of hatchetfishes on a dive off Florida. Aggregations of the lanternfish *Ceratoscopelus maderensis* were seen from the submersible *Alvin* in slope waters off the western North Atlantic (Backus *et al.*, 1968); these aggregations were about 5–10 m thick and 100 m in diameter, the same size as the small patches observed acoustically off Oregon. Such small patches, imbedded in larger-scale patches, may be common features of oceanic lanternfishes and other micronektonic animals and may have some special ecological value to these organisms.

Acknowledgments. This work was supported by the Office of Naval Research, Ocean Acoustics branch and Oceanic Biology branch, under Contract N00014-79-C-004. We are grateful for the assistance during the cruise provided by M. Willis, S. DiPiazza, F. Evans, and the crew of F/V *Victory*.

REFERENCES

Atsatt, L. H. and R. R. Seapy 1974. An analysis of sampling variability in replicated midwater trawls off southern California. J. Exp. Mar. Biol. Ecol., *14*, 261–273.

Backus, R. H., J. E. Craddock, R. L. Haedrich, D. M. Shores, J. M. Teal and A. S. Wing. 1968. *Ceratoscopelus maderensis:* peculiar sound-scattering layer identified with this myctophid fish. Science, *160*, 991–993.

Barham, E. G. 1971. Deep sea fishes: lethargy and vertical orientation, *in* Biological Sound Scattering in the Ocean, G. B. Farquhar, ed., Maury Center for Ocean Science Rpt. 005, U.S. Govt. Printing Office, 100–118.

Greenblatt, P. 1982. Distributions of volume scattering observed with an 87.5 kHz sonar. J. Acoust. Soc. Am., *71*, 879–885.

Greenlaw, C. F., R. K. Johnson and T. Pommeranz. 1979. Volume scattering strength predictions for Antarctic krill (*Euphausia superba* Dana). Meeresforsch., *28*, 48–55.

Haury, L. R., J. A. McGowan and P. H. Wiebe. 1978. Patterns and processes in the time-space scales of plankton distributions, *in* Spatial Pattern in Plankton Communities, J. H. Steele, ed., NATO Conf. Series IV: Marine Sciences, Plenum Press.

Hewitt, R. P., P. E. Smith and J. C. Brown. 1976. Development and use of sonar mapping for pelagic stock assessment in the California Current area. U.S. Fish. Bull., *74*, 281–300.

Jenkins, G. M. and D. G. Watts. 1968. Spectral Analysis and its Applications, Holden-Day (San Francisco), 525 pp.

Johnson, R. K. 1977. Acoustic estimation of scattering-layer composition. J. Acoust. Soc. Am., *61*, 1636–1639.

Pearcy, W. G. 1964. Some distributional features of mesopelagic fishes off Oregon. J. Mar. Res., *22*, 83–102.

—— 1977. Variations in abundance of sound scattering animals off Oregon, *in* Biological Sound Scattering in the Ocean, G. B. Farquhar, ed., Maury Center for Ocean Science Rep. 005, U. S. Govt. Printing Office, 647–666.

Pearcy, W. G. and R. S. Mesecar. 1971. Scattering layers and vertical distribution of oceanic animals off Oregon, *in,* Biological Sound Scattering in the Ocean, G. B. Farquhar, ed., Maury Center for Ocean Science Rep. 005, U.S. Govt. Printing Office, 381–394.

Smith, P. E. 1978. Precision of sonar mapping for pelagic fish assessment in the California Current. J. Cons. Int. Explor. Mer, *38,* 33–40.

Steele, J. H. (ed.) 1978. Spatial Pattern in Plankton Communities, NATO Conf, Series IV: Marine Sciences. Plenum Press.

Stevenson, M. R., J. G. Pattullo and B. Wyatt. 1969. Subsurface currents off the Oregon coast as measured by parachute drogues. Deep-Sea Res., *16,* 449–461.

Urick, R. J. 1967. Principles of Underwater Sound for Engineers. McGraw-Hill, NY, 337 pp.

Received: *26 January, 1984;* revised: *29 August, 1984.*